



Oblique rifting at oceanic ridges: Relationship between spreading and stretching directions from earthquake focal mechanisms

Marc Fournier, Carole Petit

► To cite this version:

Marc Fournier, Carole Petit. Oblique rifting at oceanic ridges: Relationship between spreading and stretching directions from earthquake focal mechanisms. *Journal of Structural Geology*, 2007, 29, pp.201-208. 10.1016/j.jsg.2006.07.017 . hal-00581725

HAL Id: hal-00581725

<https://hal.sorbonne-universite.fr/hal-00581725>

Submitted on 31 Mar 2011

HAL is a multi-disciplinary open access archive for the deposit and dissemination of scientific research documents, whether they are published or not. The documents may come from teaching and research institutions in France or abroad, or from public or private research centers.

L'archive ouverte pluridisciplinaire **HAL**, est destinée au dépôt et à la diffusion de documents scientifiques de niveau recherche, publiés ou non, émanant des établissements d'enseignement et de recherche français ou étrangers, des laboratoires publics ou privés.

**Oblique rifting at oceanic ridges:
Relationship between spreading and stretching directions
from earthquake focal mechanisms**

Marc Fournier, Carole Petit

CNRS UMR 7072, Laboratoire de Tectonique, Université Pierre et Marie Curie-Paris6, Case
129, 4 place Jussieu, 75252 Paris Cedex 05, France

marc.fournier@lgs.jussieu.fr

Fax: (33) 1-44-27-50-85

Abstract. The relationship between spreading and stretching directions is investigated at oblique-spreading oceanic ridges using earthquake focal mechanisms. The stretching direction at ridge axes corresponds to the direction of the greatest principal strain ϵ_1 taken as the mean trend of the seismic T-axes of extensional earthquake focal mechanisms. It is compared with the spreading direction provided by global plate-motion models. We find that the stretching direction trends approximately halfway between the spreading direction and the normal to the ridge trend, a result in line with analogue experiments of oblique rifting. This result is satisfactorily accounted for with an analytical model of oblique rifting, for which the direction of ϵ_1 is calculated with respect to rifting obliquity for different amounts of stretching using continuum mechanics. For low stretching factors, typical of incremental seismic deformations, ϵ_1 obliquity is two times lower than rifting obliquity. For higher stretching factors, the stretching and spreading directions become parallel.

Keywords: oblique rifting, oblique-spreading ridges, stretching, extension

1. Introduction

Determining the direction of relative motion between two rigid plates on either side of a deformation zone can be achieved by analysing the strain within the deformation zone. In oblique deformation settings, i.e., when the direction of displacement between the two rigid plates is oblique to the deformation zone, the direction of relative motion is generally not parallel to the principal strain directions (e.g., Sanderson and Marchini, 1984; Tikoff and Teyssier, 1994; Dewey et al., 1998; Fossen and Tikoff, 1998). This result is for example the case at the axial rifts of oblique-spreading mid-oceanic ridges (Taylor et al., 1994; Tuckwell et al., 1996), which are investigated in this paper.

The process of oblique divergence between two tectonic plates often involves the formation of an oblique rift. Oblique rifting occurs in the continental domain (e.g. Lake Baikal; Petit et al, 1996) as well as in the oceanic domain at the axis of slow-spreading ridges (e.g., Southwest Indian Ridge). The faulting and strain patterns associated with oblique rifting have been investigated for both oceanic and continental rifts (Dauteuil and Brun, 1993, 1996; Murton and Parson, 1993; Shaw and Lin, 1993; Taylor et al., 1994; Applegate and Shor, 1994; Carbotte and Mac Donald, 1994; McAllister et al., 1995; Dauteuil et al., 2001; Acocella and Korme, 2002; Clifton and Schlische, 2003; Fournier et al., 2004a), and by means of experimental (Withjack and Jamison, 1986, Tron and Brun, 1991; Dauteuil and Brun, 1993; McClay and White, 1995; Bonini et al., 1997; Clifton et al., 2000; Mart and Dauteuil, 2000; Clifton and Schlische, 2001; Venkat-Ramani and Tikoff, 2002), analytical (Elliot, 1972; Sanderson and Marchini, 1984; McCoss, 1986; Withjack and Jamison, 1986; Fossen and Tikoff, 1993; Tikoff and Fossen, 1993, 1998; Krantz, 1995; Tuckwell et al., 1996; Abelson and Agnon, 1997), and numerical (Tuckwell et al., 1998) models. These studies show that oblique rifting is accommodated by both normal and strike-slip faults, whose relative proportions and orientations depend on rifting obliquity defined as the angle between the normal to the rift trend and the direction of displacement. Oblique rifting typically produces en echelon fault patterns that are not perpendicular to the direction of relative motion.

Withjack and Jamison (1986) demonstrated, with analogue clay models marked at their surface by deformed circles, that three structural directions are linked in the process of oblique rifting: the rift trend (or its perpendicular), the direction of relative motion between the two plates, and the trend of the greatest principal strain axis ϵ_1 of the finite strain ellipsoid (Figure 1). When the direction of relative motion is perpendicular to the rift trend, the rift formation involves pure shear extension without simple shear and the deformation is accommodated by dip-slip normal faults parallel to the rift. The ϵ_1 axis is then horizontal, perpendicular to the normal faults, and parallel to the direction of divergence. When the relative motion is oblique to the rift trend, i.e., in transtensional settings, the rift formation involves a combination of pure shear extension and simple shear. The deformation is accommodated by a combination of normal faults parallel and oblique to the rift trend, and also by strike-slip faults when the rifting obliquity increases. In this case, ϵ_1 is approximately bisector of the angle between the displacement vector and the normal to the rift (Withjack and Jamison, 1986). The analytical solution to the problem of oblique rifting, based on the general theory of transpression-transtension developed by Sanderson and Marchini (1984) and Tikoff and Teyssier (1994), confirms that the infinitesimal extension direction is exactly the bisector of the angle between the displacement vector and the normal to the rift (see also McCoss, 1986).

Tron and Brun (1991) and Clifton et al. (2000) showed with laboratory experiments that the fault strike distribution in oblique rifts depended on the rifting obliquity. Consequently, a statistical analysis of fault strikes in natural rifts may provide an accurate estimate of the direction of divergence. This rule has been applied successfully to determine the direction of spreading along two slow-spreading ridges, the Mohns Ridge in the North Atlantic Ocean (Dauteuil and Brun, 1993) and the West Sheba Ridge in the Gulf of Aden (Dauteuil et al., 2001), and the kinematic evolution of the Okinawa Trough (Sibuet et al., 1995, Fournier et al., 2001a). Taylor et al. (1994) and Tuckwell et al. (1996) examined the relationship between the orientation of extensional fractures and the plate motion vector at oblique spreading ridges and at so-called “extensional transform zones” (ETZ) characterized by an obliquity between

45° and 75° (Taylor et al., 1994). They observed that, at oblique spreading ridges, most normal faults form at an angle with the ridge axis approximately equal to the half of the plate motion obliquity, a result in line with the experiments of Withjack and Jamison (1986), Tron and Brun (1991), and Clifton et al. (2000).

However, with the exception of the work of Withjack and Jamison (1986), these studies mainly focused on fault strikes and did not regard the implications in terms of strain. In experimental models as well as in the offshore domain, statistical analysis of fault distributions does not allow estimation of strain axes directions because slip vectors on fault planes cannot be directly observed. In seismically active rifts, however, the direction of maximum stretching can be inferred from earthquake focal mechanisms. In the following, we investigate the relationship between spreading and stretching directions as determined from earthquake focal mechanisms at six oblique spreading ridges.

2. Stretching direction determined from earthquake focal mechanisms

In a homogeneous and isotropic material, rupture occurs on two conjugate planes of maximum shear stress oriented with respect to the maximum and minimum stresses σ_1 and σ_3 . Because most earthquakes occur on pre-existing faults, earthquakes do not provide direct evidence for the orientation of principal stresses, but instead provide evidence for the orientation of the strain axes (e.g., Twiss and Unruh, 1998). The compression (P) and tension (T) axes of the double-couple focal mechanism solutions are defined kinematically by fault slip and correspond to the principal strain axes ϵ_3 and ϵ_1 , respectively. They represent the principal axes of the incremental (or instantaneous) strain tensor for fault movements (e.g., McKenzie, 1969; Marrett and Allmendinger, 1990). Thus, in extensional settings, T-axes of normal faulting earthquakes can be used to determine the direction of stretching. This method is applicable in regions of homogeneous deformation, i.e. when focal mechanisms are all of the same type, which is the case at spreading centres of oceanic ridges.

3. Stretching vs spreading directions at oblique spreading ridges

In the oceanic domain, rifting occurs at the crest of slow-spreading mid-oceanic ridges characterised by high seismic activity. Fast spreading centres are devoid of an axial rift and seismicity, and are characterized by orthogonal spreading except in a few back-arc basins where ETZ have been described, such as the Manus and Lau basins (Taylor et al., 1994). At fast spreading ridges, the obliquity between the spreading direction and the plate boundary is taken up by transform faults (e.g., Pacific-Antarctic Ridge). The main oblique-spreading ridges on Earth are the Southwest Indian Ridge (SWIR) in the Indian Ocean (Figure 2; Ewing and Heezen, 1960; Fisher and Sclater, 1983; Patriat, 1987), the Sheba Ridge in the Gulf of Aden (Figure 3; Matthews et al., 1967; Laughton et al., 1970), and the Reykjanes (Figure 4; Vine, 1966), Mohns (Figure 5; Talwani and Eldholm, 1977), and Knipovich (Figure 5; Vogt et al., 1979; Okino et al., 2002) ridges in the North Atlantic Ocean. These five ridges have been surveyed together with the Carlsberg Ridge in the northwest Indian Ocean (Figure 3; Schmidt, 1932; Vine and Matthews, 1963), which is generally considered as a type example of orthogonal-spreading ridge.

We have selected in the Harvard centroid moment tensor (CMT) catalog all focal mechanisms of earthquakes shallower than 50 km which occurred between 1976 and 2000 (25 years) along these six ridges (Dziewonski et al., 1981). 271 mechanisms of extensional or strike-slip type have been obtained and are plotted in Figures 2 to 5. For each ridge or ridge segment, we determined its mean trend, the mean spreading direction, and the mean stretching direction (Table 1). If necessary, the ridges have been divided in roughly rectilinear segments. For example, the SWIR has been divided into two parts: the northeastern part strikes N54°E on average and the southwestern part N105°E (Figure 2). The ridge mean trend has been directly measured on bathymetric and seismic maps. The mean spreading direction corresponds to the average of the spreading directions calculated at the ridge segment extremities from the NUVEL-1A plate motion model (DeMets et al., 1990; 1994), except for Sheba and Carlsberg ridges for which we used Fournier et al. (2001b) solution (Table 1). The mean stretching direction is computed from the normal faulting solutions (inserts in Figures 2 to 5). From these data, the spreading and stretching obliquities have been calculated for each

ridge (Table 1). Strike-slip focal mechanisms along transform faults are also plotted in Figures 2 to 5 to show the consistency between slip vectors of strike-slip mechanisms and spreading directions provided by plate motion models.

The stretching obliquity (S_{obl}) is plotted against spreading (or rifting) obliquity (R_{obl}) for the selected ridges in Figure 6. Spreading obliquities greater than 45° are never observed along slow-spreading ridges. The points plot along the $S_{obl} = R_{obl} / 2$ line for spreading obliquities less than 30° (Carlsberg, southwestern SWIR, Reykjanes, and Knipovich ridges), and slightly depart from this line for obliquities between 30° and 45° (Mohns, northeastern SWIR, and Sheba ridges).

4. Analytical model of oblique rifting

A horizontal plane-strain model of oblique rifting is presented in Figure 6a. A unit length of lithosphere (initial rift) is obliquely extended to a length β measured perpendicularly to the rift axis. β thus defines a stretching factor corresponding to the ratio of the final versus initial length (e.g., McKenzie, 1978). The stretching obliquity, defined as the angle between the normal to the rift trend and greatest principal strain axis of the strain ellipse (ϵ_1), is calculated as a function of the rifting obliquity and β .

The finite strain ellipse is calculated from continuum mechanics by decomposing the deformation matrix (deformation gradient tensor) in finite strain (shape and orientation of the strain ellipse in 2D) and finite rotation of the principal strain axes (e.g., Elliot, 1972; Jaeger and Cook, 1979; McKenzie and Jackson, 1983; Fournier et al., 2004b). The eigenvalues and eigenvectors of the finite strain matrix provide the length and orientation of the principal axes of the finite strain ellipse. Exactly the same result is obtained by factorization of the deformation matrix into pure shear and simple shear components (e.g., Sanderson and Marchini, 1986; Tikoff and Fossen, 1993; Fossen and Tikoff, 1993; Tikoff and Teyssier, 1994; Krantz, 1995; Fossen and Tikoff, 1998).

The strain ellipse resulting from oblique rifting is shown as a function of the rifting obliquity for various values of stretching factor β in Figure 6b. For a given rifting obliquity,

the principal strain axes progressively rotate as β increases. For a rifting obliquity of 45° , the stretching obliquity increases from 24° for $\beta = 1.1$ to 36° for $\beta = 3$. Furthermore, for a given β , the stretching obliquity increases as the rifting obliquity increases. For example, for $\beta = 2$, the stretching obliquity increases to 10° to 20° , 32° , 45° , and 63° for rifting obliquity of 15° to 30° , 45° , 60° , and 75° , respectively.

In Figure 6c, the stretching obliquity is plotted against rifting obliquity for various values of β . When β is small ($\beta < 1.1$), the stretching obliquity is equal to the half of the rifting obliquity ($S_{obl} = R_{obl} / 2$). With increasing strain ($\beta > 5$), the stretching obliquity becomes almost equal to the rifting obliquity ($S_{obl} = R_{obl}$).

5. Discussion

These predictions can be compared with the results obtained for the selected oblique-spreading ridges (Figure 6). For most ridges, the ε_1 direction ranges along the $S_{obl} = R_{obl} / 2$ line, which corresponds to a low amount of extension in the model. A simple interpretation is that rocks of the Earth's upper crust undergo small strains of a few per cent before brittle failure occurs and relieves the accumulated strain. The principal strain directions deduced from earthquake focal mechanisms thus represent the infinitesimal (or instantaneous) strain ellipsoid.

Our results can also be compared with those of Taylor et al. (1994) and Tuckwell et al. (1996) for the Reykjanes, Mohns, Southwest Indian (NE), and Sheba ridges, provided one converts their α and ϕ angles into rifting and stretching obliquities:

$$\begin{aligned} R_{obl} &= 90 - \alpha \\ S_{obl} &= \phi - \alpha \end{aligned}$$

In contrast with us, Taylor et al. (1994) and Tuckwell et al. (1996) defined the stretching direction as the perpendicular to the mean trend of normal faults in extension zones.

We find a very good agreement for the Reykjanes Ridge, where our estimates of spreading and stretching obliquities differ only by 1° and 4° , respectively, which is smaller than the uncertainties. For the Mohns Ridge, our results compare well with those of Taylor et

al. (1994) but slightly differ from Tuckwell et al. (1996) estimates of spreading obliquity ($34\pm 8^\circ$ vs $40\pm 6^\circ$), mainly because we (and Taylor et al., 1994) use a different azimuth of spreading ($N119^\circ E$ vs $N110^\circ E$). Despite this, we find no large discrepancies between our estimates of stretching obliquity and theirs. Much larger differences are found for the Southwest Indian and Sheba ridges: for the former, whereas Taylor et al. (1994) and Tuckwell et al. (1996) give comparable values of 14° and $23-27^\circ$ for stretching and spreading obliquities, we find $29\pm 7^\circ$ and $42\pm 11^\circ$, respectively. These differences are entirely attributable to different estimates of ridge trend and spreading directions, due to the fact that Taylor et al. (1994) and Tuckwell et al. (1996) took into account only a small part of the SWIR located near the Rodrigues triple junction ($26^\circ N$; Mitchell, 1991), whereas we have taken into account all the northeastern part of the SWIR over several thousands kilometres (Figure 2). However, here again, the determination of stretching directions from earthquake focal mechanisms gives results comparable to the analysis of normal fault trends. Concerning the Gulf of Aden (Sheba Ridge), a difference up to $5-10^\circ$ exists between our values and those of Taylor et al. (1994) and Tuckwell et al. (1996). Once again, these differences come from the selection of different study areas. The results of Taylor et al. (1994) and Tuckwell et al. (1996) concern the westernmost part of the Sheba Ridge near the Gulf of Tadjura ($45^\circ E$; Tamsett and Searle, 1988), whereas our results encompass the entire ridge from $46^\circ E$ to $56^\circ E$ (Figure 3; Table 1). Hence, the differences between our results and those of Taylor et al. (1994) and Tuckwell et al. (1996) come from different scales of study. Studying normal fault strikes at ridge axes requires detailed mapping of fault fabrics. Working with focal mechanisms from the world seismicity catalogs allows surveying of larger areas.

In general, the results of Tuckwell et al. (1996) show that most values of stretching vs rifting obliquities range along the $S_{obl} = R_{obl} / 2$ line, like in the present study. Surprisingly, the direction of ϵ_1 deduced from infinitesimal strain (earthquakes) does not differ from the perpendicular to the normal faults, which are markers of finite strain and can have accommodated a significant amount of deformation. This result suggests that normal faults initially form perpendicular to the direction of ϵ_1 of the infinitesimal strain ellipsoid, keep this

orientation during ongoing extension, and do not significantly rotate as the strain increases. As oblique slip (characterized by oblique focal mechanisms) is seldom observed, this implies that normal faults at ridge axes only accommodate a small amount of deformation during the time when they are located in the seismically active part of the rift (about 2 Ma for a ridge with a half-spreading rate of 5 mm/yr and a 20 km large axial rift).

6. Conclusion

Plate-motion models such as RM2 and NUVEL-1 (Minster and Jordan, 1978; DeMets et al., 1990) did not account for slip vectors of extensional focal mechanisms along oceanic ridges. The first reason was of course that, for extensional mechanisms, it is not possible to determine which of the two nodal planes is the fault plane and which is the actual slip vector. The second reason was that at oblique-spreading ridges, slip vectors are not parallel but oblique to the plate relative motion. Here, we demonstrate that, at slow-spreading oblique ridges, the maximum strain axis determined from earthquake focal mechanisms trends halfway between the direction of spreading and the normal to the ridge. Hence, the kinematics of oblique ridges and rifts can possibly be determined from a set of extensional focal mechanisms, without assumption on the fault plane and the slip vector. This result could be useful in continental rifts where transform faults are not developed and plate kinematics difficult to assess. The comparison with an analytical model of oblique rifting shows that these features correspond to small deformations at ridge axes, which is consistent with the fact that earthquakes represent infinitesimal strains. Furthermore, the analysis of normal faults directions (Taylor et al., 1994; Tuckwell et al., 1996) yields similar conclusions, though normal fault heaves represent thousands of co-seismic slips. Yet, compared to the rift width (~10 to 20 km), the cumulated stretching factor on each fault must remain low.

Acknowledgments. We are grateful to the Editor W. Dunne and to D. Sanderson and B. Tikoff for their constructive reviews of the manuscript. We thank E. Coudret for valuable

246 discussions at the initiation of this work. Figures were drafted using GMT software (Wessel
247 and Smith, 1991).

References

- Abelson, M., Agnon, A., 1997. Mechanics of oblique spreading and ridge segmentation. *Earth Planetary Science Letter* 148, 405-421.
- Acocella, V., Korme, T., 2002. Holocene extension direction along the Main Ethiopian Rift, East Africa. *Terra Nova* 14, 191-197.
- Appelgate, B., Shor, A. N., 1994. The northern Mid-Atlantic and Reykjanes Ridges: Spreading center morphology between 55°50'N and 63°00'N. *Journal of Geophysical Research* 99, 17,935-17,956.
- Bonini, M., Souriot, T., Boccaletti, M., Brun, J.-P., 1997. Successive orthogonal and oblique extension episodes in a rift zone: Laboratory experiments with application to the Ethiopian Rift. *Tectonics* 16, 347-362.
- Carbotte, S. M., Macdonald, K. C., 1994. Comparison of seafloor tectonic fabric at intermediate, fast, and super fast spreading ridges: Influence of spreading rate, plate motions, and ridge segmentation on fault patterns. *Journal of Geophysical Research* 99, 13,609-13,632.
- Clifton, A.E., Schlische, R.W., 2003. Fracture populations on the Reykjanes Peninsula, Iceland: Comparison with experimental clay models of oblique rifting. *Journal of Geophysical Research* 108, 1-17.
- Clifton, A.E., Schlische, R.W., 2001. Nucleation, growth, and linkage of faults in oblique rift zones: Results from experimental clay models and implications for maximum fault size. *Geology* 29, 455-458.
- Clifton, A.E., Schlische, R.W., Withjack, M.O., Ackermann, R.V., 2000. Influence of rift obliquity on fault-population systematics: results of experimental clay models. *Journal of Structural Geology* 22, 1491-1509.
- Dauteuil, O., Brun, J.P., 1996. Deformation partitioning in a slow-spreading ridge undergoing oblique extension (Mohs Ridge, Norwegian Sea). *Tectonics* 17, 303-310.
- Dauteuil, O., Brun, J.P., 1993. Oblique rifting in a slow-spreading ridge. *Nature* 361, 145-148.

- 276 Dauteuil, O., Huchon, P., Quemeneur, F., Souriot, T., 2001. Propagation of an oblique
277 spreading centre: the western Gulf of Aden. *Tectonophysics* 332, 423-442.
- 278 DeMets, C., Gordon, R.G., Argus, D.F., Stein, S., 1990. Current plate motion. *Geophysical*
279 *Journal International* 101, 425-478.
- 280 DeMets, C., Gordon, R.G., Argus, D.F., Stein, S., 1994. Effects of recent revisions to the
281 geomagnetic reversal time scale on estimates of current plates motions. *Geophys. Res.*
282 *Lett.* 21, 2191-2194.
- 283 Dewey J.F., Holdsworth, R.E., Strachan, R.A., 1998. Transpression and transtension zones.
284 *In: Holdsworth, R.E., Strachan, R.A. & Dewey, J.F. (eds) Continental Transpressional*
285 *and Transtensional Tectonics*. Geological Society, London, Special Publications 135, 1-
286 14.
- 287 Dziewonski, A. M., Chou, T. A., Woodhouse, J. H., 1981. Determination of earthquake
288 source parameters from waveform data for studies of global and regional seismicity.
289 *Journal of Geophysical Research* 86, 2825-2852.
- 290 Elliott, D., 1972. Deformation paths in structural geology. *Geol. Soc. America Bull.* 83, 2621-
291 2638.
- 292 Engdahl, E.R., van der Hilst, R., Buland, R., 1998. Global teleseismic earthquake relocation
293 with improved travel times and procedures for depth determination. *Bulletin of the*
294 *Seismological Society of America* 88, 722-743.
- 295 Ewing, M., Heezen, B. C., 1960. Continuity of mid-oceanic ridge and rift valley in the
296 southwestern Indian Ocean confirmed. *Science*, 131, 1677-1679.
- 297 Fisher, R.L., Sclater, J.G., 1983. Tectonic evolution of the Southwest Indian Ocean since the
298 mid-Cretaceous: plate motions and stability of the pole of Antarctica-Africa for at least 80
299 Myr. *Geophysical Journal of the Royal Astronomical Society* 73, 553-576.
- 300 Fossen, H., Tikoff, B., 1993. The deformation matrix for simultaneous simple shearing, pure
301 shearing and volume change, and its application to transpression-transtension tectonics. *J.*
302 *Struct. Geol.* 3-5, 413-422.

- 303 Fossen, H., Tikoff, B., 1998. Extended models of transpression and transtension, and
 304 application to tectonic settings. *In*: Holdsworth, R.E., Strachan, R.A. & Dewey, J.F. (eds)
 305 *Continental Transpressional and Transtensional Tectonics*. Geological Society, London,
 306 Special Publications 135, 1-14.
- 307 Fournier, M., Bellahsen, N., Fabbri, O., Gunnell, Y., 2004a. Oblique rifting and segmentation
 308 of the NE Gulf of Aden passive margin. *Geochemistry Geophysics Geosystems*, 5,
 309 Q11005, doi:10.1029/2004GC000731.
- 310 Fournier, M., Fabbri, O., Angelier, J., Cadet, J.P., 2001a. Kinematics and timing of opening
 311 of the Okinawa Trough: Insights from regional seismicity and onland deformation in the
 312 Ryukyu arc. *Journal of Geophysical Research* 106, 13,751-13768.
- 313 Fournier, M., Jolivet, L., Davy, P., Thomas, J. C., 2004b. Back arc extension and collision: an
 314 experimental approach of the tectonics of Asia. *Geophys. J. Int.* 157, 871-889.
- 315 Fournier, M., Patriat, P., Leroy S., 2001b. Reappraisal of the Arabia-India-Somalia triple
 316 junction kinematics. *Earth Planetary Science Letter* 184, 103-114.
- 317 Grindlay, N. R., Madsen, J. A., Rommevaux-Jestin, C., Sclater, J., 1998. A different pattern
 318 of ridge segmentation and mantle Bouguer gravity anomalies along the ultra-slow
 319 spreading Southwest Indian Ridge (15°30'E to 25°E). *Earth Planetary Science Letter* 161,
 320 243-253.
- 321 Jaeger, J.C., Cook, N.G.W., 1979. *Fundamentals of rocks mechanism*. Third Edition,
 322 Chapman and Hall, London.
- 323 Krantz, R.W., 1995. The transpressional strain model applied to strike-slip, oblique-
 324 convergent and oblique-divergent deformation. *J. Struct. Geol.* 17, 1125-1137.
- 325 Laughton, A.S., Whitmarsh, R.B., Jones M.T., 1970. The evolution of the Gulf of Aden.
 326 *Philos. Trans. R. Soc. London*, A267. 227-266.
- 327 Marrett, R., Allmendinger, R.W., 1990. Kinematic analysis of fault-slip data. *Journal of*
 328 *Structural Geology* 12, 973-986.
- 329 Mart, Y., Dauteuil, O., 2000. Analogue experiments of propagation of oblique rifts.
 330 *Tectonophysics* 316, 121-132.

- 331 Matthews, D. H., Williams, C., Laughton, A. S., 1967. Mid-ocean ridge in the mouth of the
332 Gulf of Aden. *Nature*, 215, 1052-1053.
- 333 McAllister, E., Cann, J., Spencer, S., 1995. The evolution of crustal deformation in an
334 oceanic extensional environment. *Journal of Structural Geology* 17, 183-199.
- 335 McClay, K. R., White, M. J., 1995. Analogue modelling of orthogonal and oblique rifting.
336 *Marine and Petroleum. Geology* 12, 137-151.
- 337 McCoss, A.M. 1986. Simple constructions for deformation in transpression/transtension
338 zones. *Journal of Structural Geology* 8, 715-718.
- 339 McKenzie, D. P., 1969. The relationship between fault plane solutions for earthquakes and the
340 directions of the principal stresses. *Bull. Seism. Soc. America* 59, 591-601.
- 341 McKenzie, D.P., 1978. Some remarks on the development of sedimentary basins. *Earth*
342 *Planet. Sci. Lett.*, 40, 25-32.
- 343 McKenzie, D. P., Jackson, J., 1983. The relationship between strain rates, crustal thickening,
344 paleomagnetism, finite strain and fault movements within a deforming zone. *Earth*
345 *Planetary Science Letter* 65, 182-202.
- 346 Minster, J.B., Jordan, T.H., 1978. Present-day plate motions. . *Journal of Geophysical*
347 *Research* 83, 5331-5354.
- 348 Mitchell, N.C., 1991. Distributed extension at the Indian Ocean triple junction. *Journal of*
349 *Geophysical Research* 96, 8019-8043.
- 350 Murton, B. J., Parson, L. M., 1993. Segmentation, volcanism and deformation of oblique
351 spreading centres: A quantitative study of the Reykjanes Ridge. *Tectonophysics*, 222, 237-
352 257.
- 353 Okino, K., Curewitz, D., Asada, M., Tamaki, K., Vogt, P., Crane, K., 2002. Segmentation of
354 the Knipovich Ridge implication for focused magmatism and effect of ridge obliquity at an
355 ultraslow spreading system. *Earth Planetary Science Letter* 202, 275-288.
- 356 Patriat, P., 1987. Reconstitution de l'évolution du système de dorsales de l'Océan Indien par
357 les méthodes de la cinématique des plaques, Territoire des Terres Australes et Antarctique
358 Françaises (ed.), 308 p., PhD Thesis, Université de Paris VI, France.

- 359 Petit, C., Déverchère, J., Houdry, F., San'kov, V.A., Melnikova, V. I., Delvaux, D., 1996.
 360 Present-day stress field changes along the Baikal rift and tectonic implications. *Tectonics*
 361 15, 1171-1191.
- 362 Sanderson, D. J., Marchini, W. R. D., 1984. Transpression. *Journal of Structural Geology* 6,
 363 449-458.
- 364 Sandwell, D.T., Smith, W.H.F., 1997. Marine gravity anomaly from Geosat and ERS-1
 365 satellite altimetry. *Journal of Geophysical Research* 102, 10039-10054.
- 366 Schmidt, J., 1932. Dana's Tugt Omkring Jorden, 1928-1930. Gyldendal ed., Copenhagen, 269
 367 pp.
- 368 Shaw, P.R., Lin, J., 1993. Causes and consequences of variations in faulting style at the Mid-
 369 Atlantic ridge. *Journal of Geophysical Research* 98, 21,839-21,851.
- 370 Sibuet, J.C., Hsu, S.-K., Shyu, C.T., Liu, C.S., 1995. Structural and kinematic evolutions of
 371 the Okinawa Trough backarc basin. In: *Backarc Basins: Tectonics and Magmatism*, edited
 372 by B. Taylor, pp. 343-379, Plenum, New York.
- 373 Talwani, M., Eldholm, O., 1977. Evolution of the Norwegian-Greenland Sea. *Geological*
 374 *Society of America Bulletin* 88, 969-999.
- 375 Tamsett, D., Searle, R., 1988. Structure of the Alula-Fartak fracture zone, Gulf of Aden.
 376 *Journal of Geophysical Research* 95, 1239-1254.
- 377 Taylor, B., Crook, K., Sinton, J., 1994. Extensional transform zones and oblique spreading
 378 centers. *Journal of Geophysical Research* 99, 19,707-19,718.
- 379 Tikoff, B., Fossen, H., 1993. Simultaneous pure and simple shear: the unifying deformation
 380 matrix. *Tectonophysics* 217, 267-283.
- 381 Tikoff, B., Teyssier, C., 1994. Strain modeling of displacement-field partitioning in
 382 transpression orogens. *Journal of Structural Geology* 16, 1575-1588.
- 383 Tron, V., Brun, J.-P., 1991. Experiments on oblique rifting in brittle-ductile systems.
 384 *Tectonophysics* 188, 71-84.
- 385 Tuckwell, G.W., Bull, J.M., Sanderson, D.J., 1996. Models of fracture orientation at oblique
 386 spreading centres. *Journal of the Geological Society London* 153, 185-189.

- 387 Tuckwell, G.W., Bull, J.M., Sanderson, D.J., 1998. Numerical models of faulting at oblique
388 spreading centers. *Journal of Geophysical Research* 103, 15474-15482.
- 389 Twiss, R.J., Unruh, J.R., 1998. Analysis of fault slip inversions: Do they constrain stress or
390 strain rates? *J. Geophys. Res.* 103, 12205-12222.
- 391 Venkat-Ramani, M., Tikoff, B., 2002. Physical models of transtensional folding. *Geology* 30,
392 523–526.
- 393 Vine, F. J., 1966. Spreading of the ocean floor; new evidence. *Science* 154, 1405-1415.
- 394 Vine, F. J., Matthews, D. H., 1963. Magnetic anomalies over oceanic ridges. *Nature* 199, 947-
395 949.
- 396 Vogt, P.R., Taylor, P.T., Kovacs, L.C., Johnson, G.L., 1979. Detailed aeromagnetic
397 investigation of the Arctic Basin. *Journal of Geophysical Research* 84, 1071-1089.
- 398 Wessel, P., Smith, W. M. F., 1991. Free software helps map and display data. *Eos Trans.*
399 AGU, 72 (41), 441-446.
- 400 Withjack, M. O., Jamison, W.R., 1986. Deformation produced by oblique rifting.
401 *Tectonophysics* 126, 99-124.

Figure captions

Figure 1. Geometrical relationship between the main structural directions at oblique rifts.

Figure 2. Bathymetric map (Sandwell and Smith, 1997), shallow seismicity between 1964 and 1995 (focal depth < 50 km; magnitude > 2; Engdahl et al., 1998), and all available earthquake focal mechanisms (Harvard CMT for the period 1976-2000; Dziewonski et al., 1981) for the Southwest Indian Ridge (SWIR). Inserted stereoplots are equal-area projections of the P and T axes of the extensional focal mechanisms and the mean direction of extension (ϵ_1). The SWIR has been divided into two parts with different trends: the northeastern part between the Rodrigues triple junction and the Prince Edward-Marion-Andrew Bain fracture zone (PEMABFZ; Grindlay et al., 1998) trends $N054^\circ E \pm 2^\circ$, and the southwestern part between PEMABFZ and $53^\circ S, 14^\circ E$ trends $N105^\circ E \pm 2^\circ$. Bathymetric contour interval is 1000m. Strike-slip focal mechanisms along fracture zones show the consistency between slip vector azimuths and directions of relative motion (solid arrows) calculated from plate motion models.

Figure 3. Same legend as Figure 2 for the Sheba and Carlsberg ridges. OTF is Owen transform faults. Bathymetric contour interval is 500m.

Figure 4. Same legend as Figure 2 for the Reykjanes Ridge. Between $55.5^\circ N, 35.5^\circ W$ and $63.5^\circ N, 24^\circ W$, the ridge strikes $N037^\circ E \pm 3^\circ$. Bathymetric contour interval is 500m.

Figure 5. Same legend as Figure 2 for the Mohns and Knipovich ridges (location in Figure 4). The Mohns Ridge strikes $N063^\circ E \pm 2^\circ$ on average between $71^\circ N, 7.5^\circ W$ and $73.5^\circ N, 8^\circ E$. The mean trend of the Knipovich Ridge between $73.7^\circ N, 9^\circ E$ and $78^\circ N, 8^\circ E$ is $N178^\circ E \pm 2^\circ$. Bathymetric contour interval is 200m.

429 Figure 6. Stretching obliquity S_{obl} (maximum principal strain ϵ_1) as a function of spreading
 430 obliquity R_{obl} in degrees for seven oblique-spreading ridges. Data sources and abbreviations
 431 are given in Table 1. See text for additional explanation. Error bars for spreading obliquity
 432 represent the sum of the uncertainties in the measurement of the ridge mean trend and in the
 433 azimuth of spreading calculated along the ridge. Error bars for stretching obliquity represent
 434 the standard deviation of the T-axes azimuth.

435

436 Figure 7. a. Plane-strain analytical model of oblique rifting. See text for additional
 437 explanation. b. Strain ellipse for various stretching factors and rifting obliquities. c.
 438 Stretching obliquity S_{obl} as a function of rifting obliquity R_{obl} in degrees. The curves are
 439 calculated from the analytical model and the straight lines correspond to $S_{obl} = R_{obl}$ and
 440 $S_{obl} = R_{obl} / 2$.

Figure

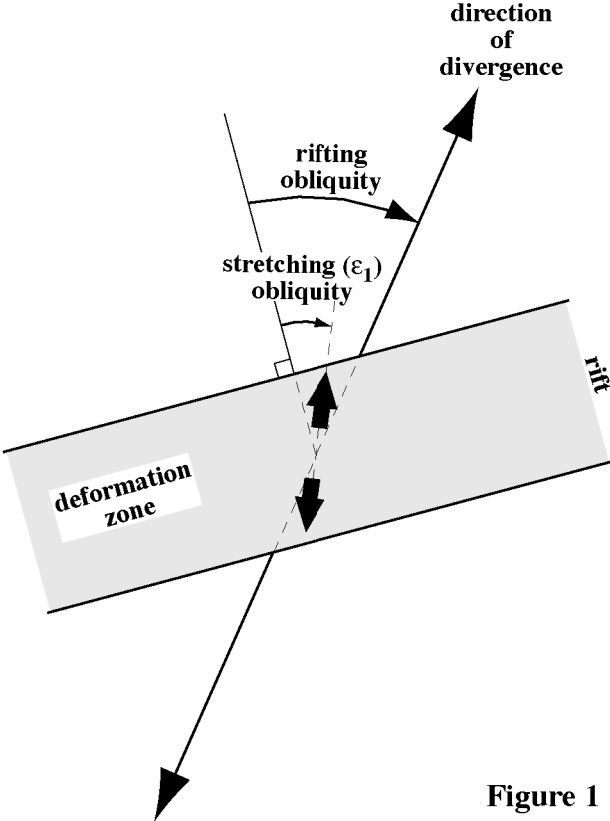


Figure 1

Figure

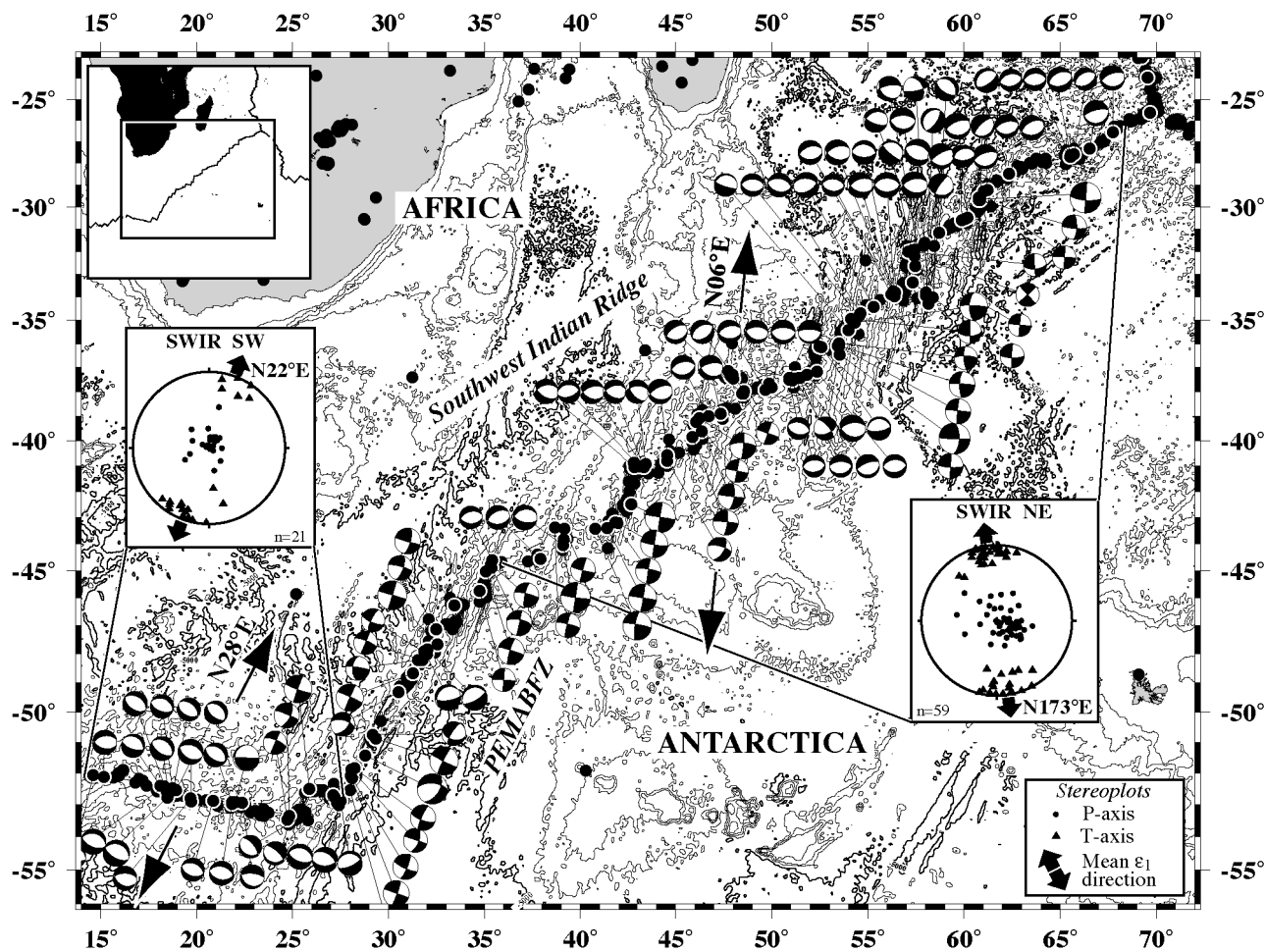


Figure 2

Figure

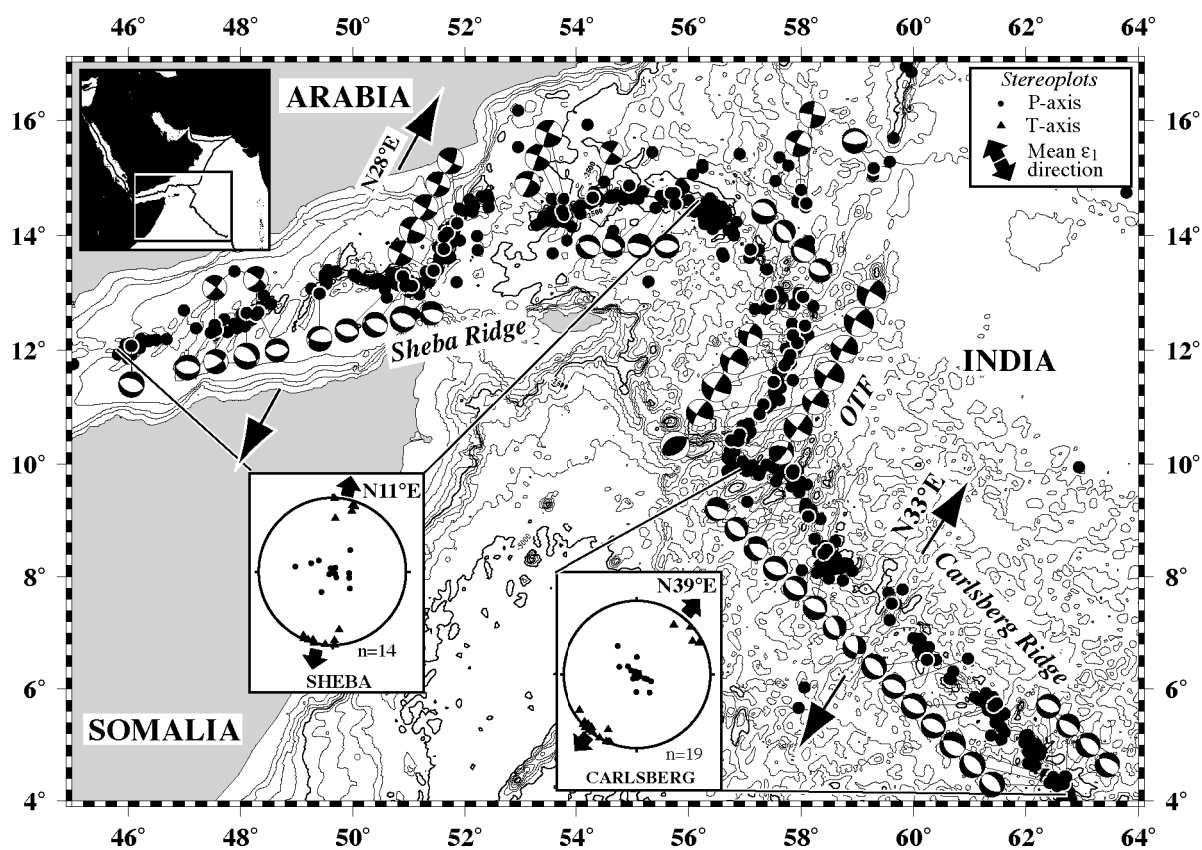


Figure 3

Figure

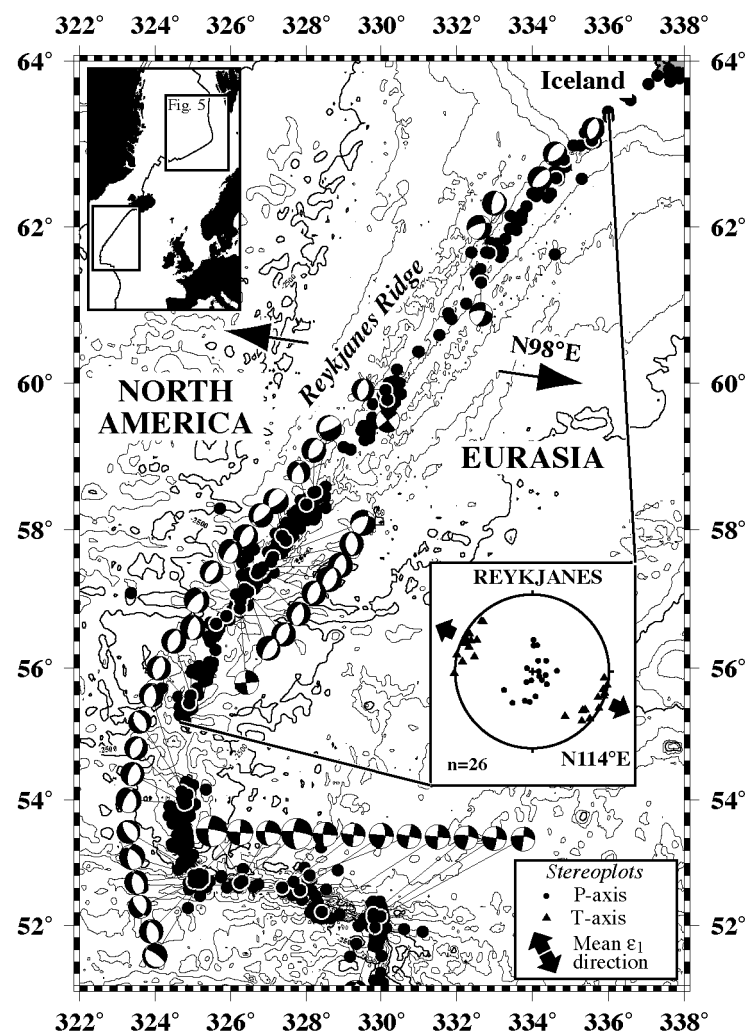


Figure 4

Figure

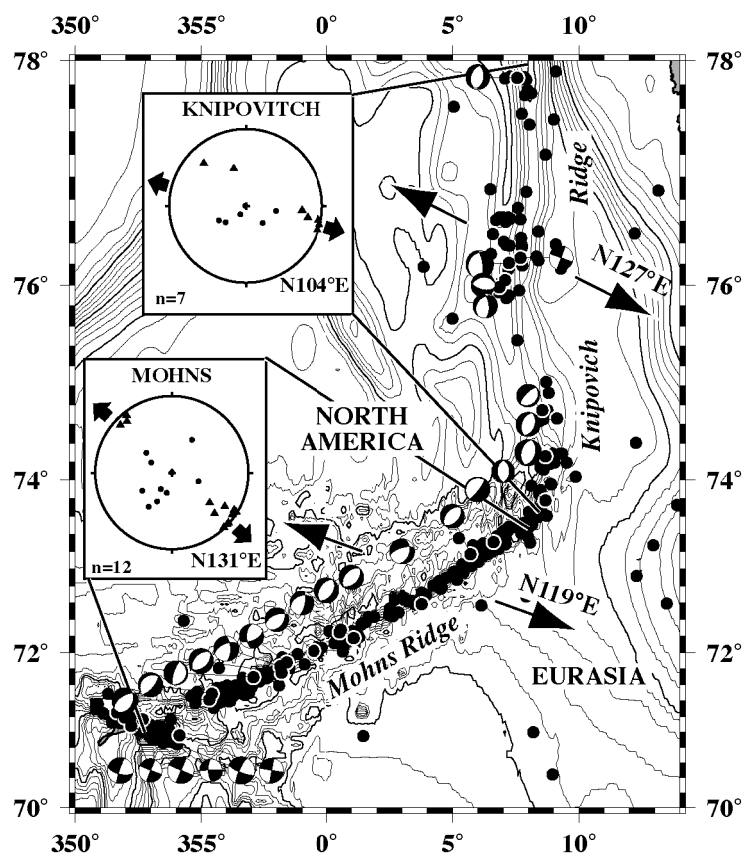


Figure 5

Figure

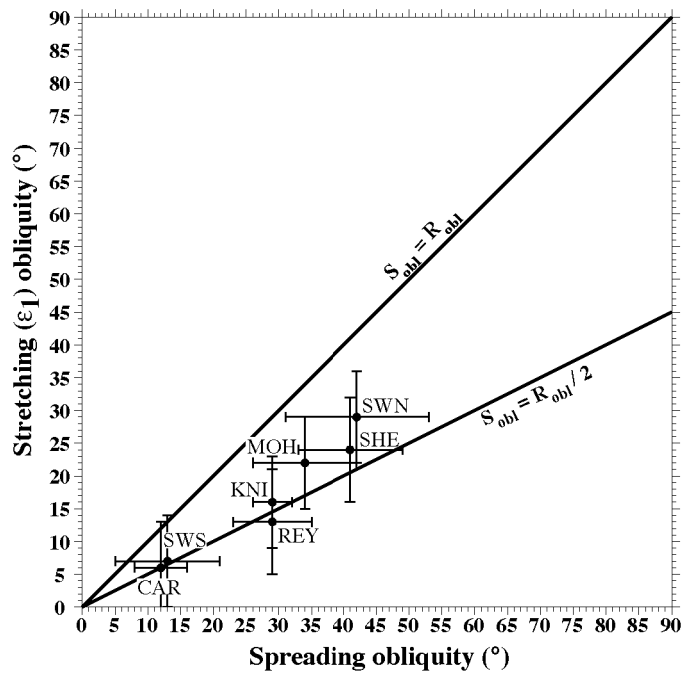


Figure 6

Figure

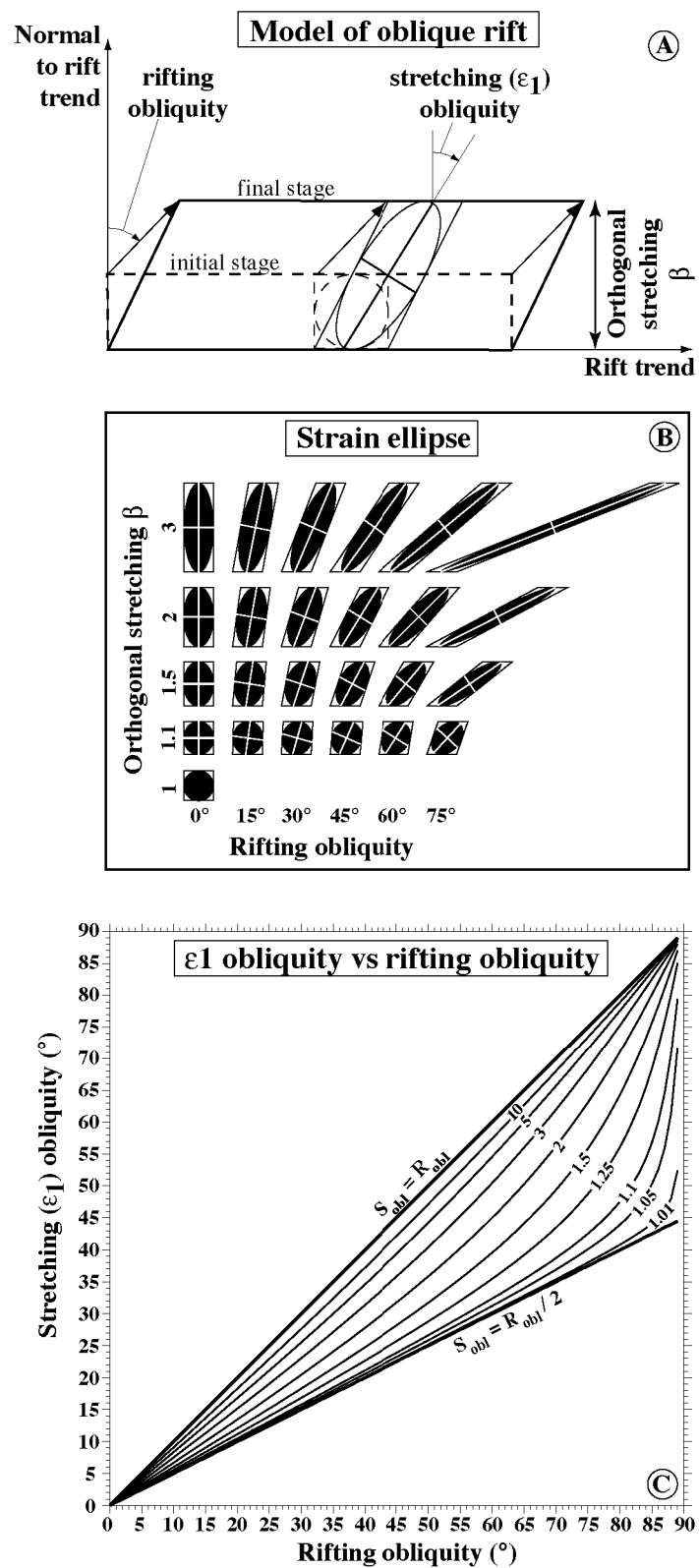


Figure 7

Table 1. Mean trend, azimuth of spreading, spreading obliquity, and principal strain ϵ_1 obliquity for oblique spreading ridges

Ridge	Ridge mean trend	Ridge extremities			Mean azimuth of spreading	Mean T-axis Strike, Dip	Spreading obliquity	Principal strain ϵ_1 obliquity	Labels ²
		Latitude	Longitude	Azimuth of spreading ¹					
		(°N)	(°E)	(°E)		deg	deg	deg	
Aden - Sheba	N077°E $\pm 3^\circ$	12	46	33	028 ± 5	011, 1 (n=14)	41 ± 8	24 ± 8	SHE
		14.5	56	23					
Carlsberg	N135°E $\pm 2^\circ$	10	57	31	033 ± 2	219, 0 (n=18)	12 ± 4	6 ± 7	CAR
		4	63	35					
SWIR NE	N054°E $\pm 2^\circ$	-45	35	15	006 ± 9	353, 3 (n=59)	42 ± 11	29 ± 7	SWN
		-26	69	177					
SWIR SW	N105°E $\pm 2^\circ$	-52	14	34	028 ± 6	202, 4 (n=21)	13 ± 8	7 ± 7	SWS
		-53	28	22					
Reykjanes	N037°E $\pm 3^\circ$	55.5	-35.5	95	098 ± 3	294, 2 (n=26)	29 ± 6	13 ± 8	REY
		63.5	-24	102					
Mohn	N063°E $\pm 2^\circ$	71	-7.5	113	119 ± 6	131, 4 (n=12)	34 ± 8	22 ± 7	MOH
		73.5	8	125					
Knipovitch	N178°E $\pm 2^\circ$	73.7	9	126	127 ± 1	104, 4 (n=7)	29 ± 3	16 ± 7	KNI
		78	8	128					

n is the number of extensional earthquake focal mechanisms used to determined the mean T-axes azimuth.

¹Azimuths of spreading after DeMets et al. (1990), except for SHE and CAR after Fournier et al. (2001).

²Labels are for data plotted in Figure 5.